Electronic Supplementary Material (ESI) for Journal of Materials Chemistry A.

Direct Solar-to-Hydrogen Generation by Quasi Artificial Leaf Approach: Possibly Scalable and Economical Device

Kshirodra Kumar Patra,[†a] Pradnya Arunrao Bharad,[†a] Vanshika Jain[a] and Chinnakonda S. Gopinath[a,b*]

[a]Catalysis Division, National Chemical Laboratory, Dr. Homi Bhabha Road, Pune 411 008, India.

[b]Centre of Excellence on Surface Science, CSIR-National Chemical Laboratory, Dr Homi Bhabha Road, Pune 411008, India.

[†]Equal First authors;

[*]Author for correspondence. Email: cs.gopinath@ncl.res.in; Fax: 0091-20-25902633

Electronic Supplementary Information (ESI)

TS1: Synthesis of NiCu bimetallic nanoparticles

The following procedure describes the synthesis of NiCu nanoparticles. 25 mL of oleylamine was taken in a round bottom flask and heated up to 120°C. Required amount of nickel (II) nitrate hexahydrate, $Ni(NO_3)_2.6H_2O$ and copper (II) acetate monohydrate, $Cu(ac)_2.H_2O$ was added to this preheated oleylamine. The reaction mixture was magnetically stirred for an hour at 220℃ . The colour of the solution changed from green to black, indicating the formation of nanoparticles. The black solution was cooled to room temperature and then the nanoparticles formed were separated by centrifugation. NiCu nanomaterial alloy was washed with ethanol and centrifuged; this procedure was repeated three times. Four different type of compositions Ni, $Ni_5Cu_{1.25}$, $Ni_5Cu_{2.5,}$ $Ni_5Cu_{3.75}$, and Ni_5Cu_5 were prepared by varying the amount of Cu, keeping Ni amount fixed. The $Ni_5Cu_{2.5}$ bimetallic NPs were also synthesized by adding 1 mmol of $Ni(NO_3)_2.6H_2O$ and 0.5mmol of $Cu(ac)_2.H_2O$ to oleylamine at 120°C.The reaction mixture was kept under stirring for 30 min at 120°C and then increase the temperature to 220°C. After reaching 220°C, the reaction mixture was kept under stirring for 1 hour. Then the as synthesized NiCu bimetallic NPs were washed, like alloy.

Schematic representation of $Ni_5Cu_{2.5}$ alloy and bimetallic synthesis.

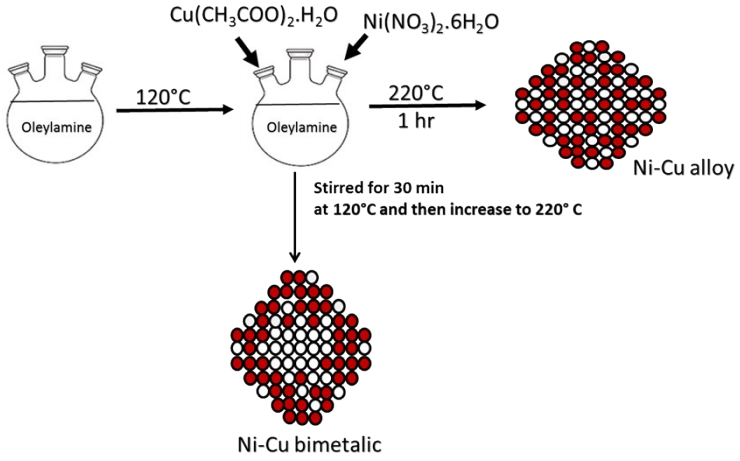

TS2: Experimental details

Calculation of PEC

The PEC of the solar driven hydrogen generation efficiency was calculated by the following equation

$$\eta = \frac{2 \times 0.21(V) \times N_{H2}(mol) \times 96485(C.mol^{-1})}{I(W.cm^{-2}) \times A(cm^2) \times t(sec)} \times 100\%$$

where N_{H2} is the amount of evolved H_2 gas, A is the area of the electrode exposed to the light, I is the intensity of light and t is the time of reaction and 0.21V represents the thermodynamic reaction potential for oxidation of sacrificial reagent.

Electrochemical characterization

The catalyst ink was prepared by taking 5 mg of NiCu catalyst and dispersed in 1 ml ofethanol-water solution (80/20 v/v). Next, 40 µl of nafion solution was added and ultra-sonicated for 30 min. Then 5 µl of the dispersion was transferred onto the glassy carbon electrode acting as a working electrode. All the electrochemical characterizations were performed on Gamry Reference 3000 potentiostat. The references electrode was Ag/AgCl (saturated KCl) purchased from CH instruments and the counter electrode was a Pt foil. All potential reported in this paper for electrochemical methods were referenced to a reversible hydrogen electrode by adding a value of (0.197 + 0.059 x pH) V. Electrochemical impedance spectroscopy data were collected in a frequency range of 10^6 Hz - 1 Hz at an HER over potential of 130 mV vs RHE

Movie 1:

Hydrogen generation video:

Movie/video (NiCu-H2.avi) for Hydrogen generation under one sun conditions with no applied bias (or wireless configuration).

S1: TEM studies of NiCu alloy NPs.

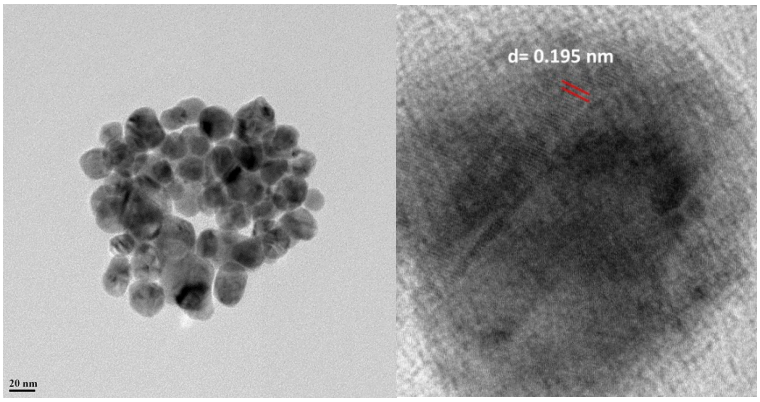

Figure S1: TEM image of $Ni_5Cu_{2.5}$ alloy NPs is shown. An enlarged view of a NP is shown in panel b and the d spacing of 0.195 nm corresponding to (111) facet of the $Ni_5Cu_{2.5}$ alloy NP. The particle size of alloy NPs is ~15 nm.

S2: SEM-EDX studies of TiO_2/Mn-CdS photoanode

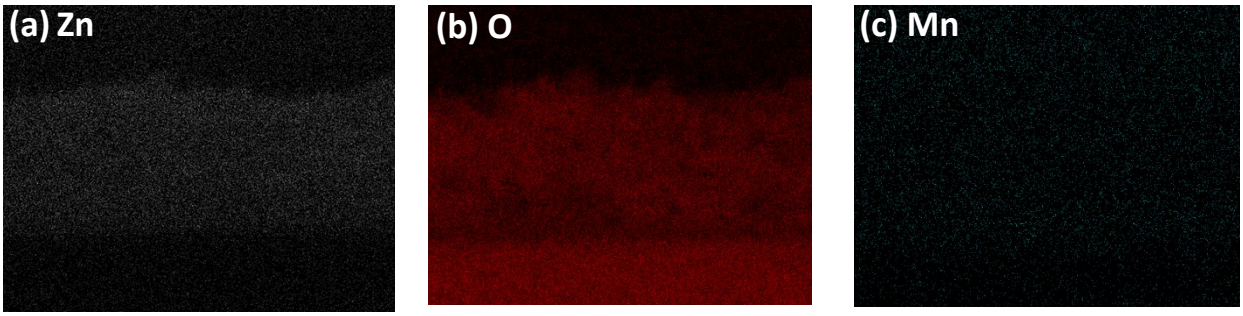

Figure S2: Chemical mapping analysis of TiO_2/Mn-CdS photoanode (a) Zn, (b) O and (c) Mn. Only in the case of Mn the difference between background noise and the Mn signal is low due to very low Mn-contet; however, a careful examination of the image in Fig. S2c reveals the presence of Mn in the photoanode. Uniform distribution of chalcogenide components underscores the bulk heterostructure available in the photoanode.

S3: X-ray Diffraction Studies

XRD pattern recorded for TiO_2, TiO_2/CdS, TiO_2/Mn-CdS is shown in Figure S3. The characteristics peaks of anatase and rutile features are present in TiO_2 and they are indexed (JCPDSFile 21-1272, 21-1276 respectively). In the composite photoanodes the crystallographic facets of TiO_2 remain as such after composite formation. For the composite, TiO_2/CdS, TiO_2/Mn-CdS there is no CdS diffraction feature was observed other than TiO_2 peaks. No CdS features was detected in XRD and it is attributed to very low concentration (0.44 wt %) of CdS in the composite. This indicates the crystallite and particle size of CdS as well as Mn-doped CdS is very small and dispersed very well.

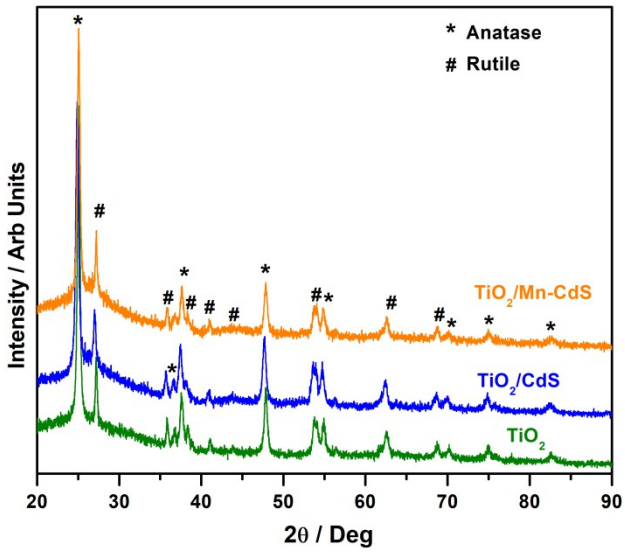

Figure S3: XRD pattern for TiO_2, TiO_2/CdS, TiO_2/Mn-CdS. No CdS diffraction feature was observed in the latter photoanodes suggesting the small size CdS and its uniform dispersion.

S4: Raman Spectral Studies

Raman spectra for TiO_2, TiO_2/CdS and TiO_2/Mn-CdS is shown in Figure S4.The fundamental modes of TiO_2 are observed around 145 (E_g),196 (E_g), 397 (B_{1g}), 516 (A_{1g} + B_{1g}), and 640 (E_g) cm^{-1} for the anatase phase and two typical rutile features at 430 (E_g) and 700 (A_{1g}) cm^{-1} is also present in all the composite materials. In the case of TiO_2/CdS and TiO_2/Mn-CdS there is no extra feature for CdS or Mn-CdS is present in the composites. However, a significant decrease in the intensity along with broadening of Raman features is observed.

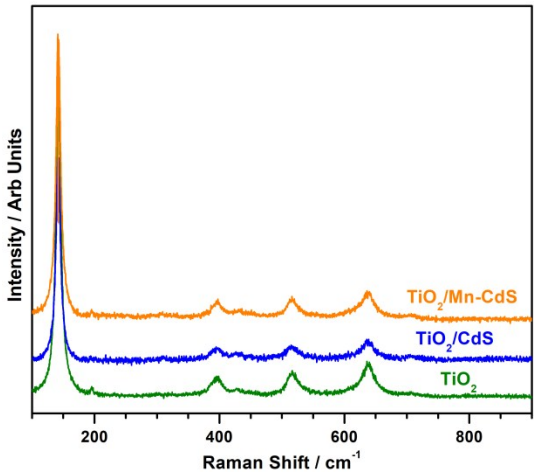

Figure S4: Raman Spectra for TiO_2, TiO_2/CdS, TiO_2/Mn-CdS

S5: XPS for Cu 2p core level in NiCu co-catalysts

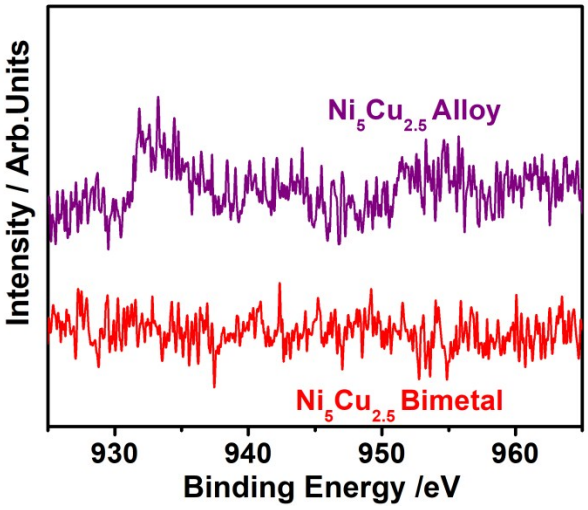

Figure S5: XPS results for Cu 2p, core levels recorded with $Ni_5Cu_{2.5}$ alloy and $Ni_5Cu_{2.5}$ bimetallic NPs.

S6: UVPES valence band spectra of NiCu co-catalysts

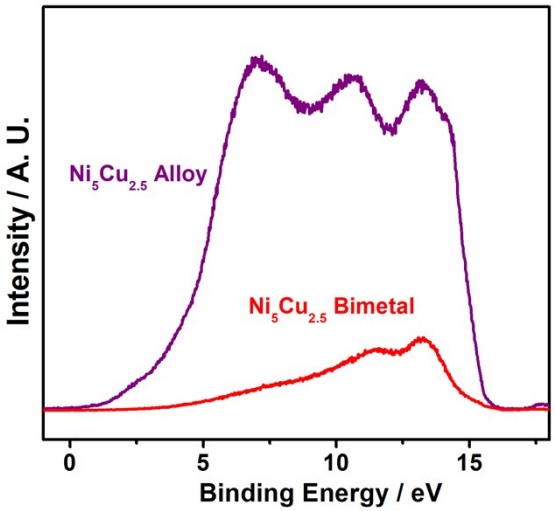

Figure S6: UVPES plot of as synthesized $Ni_5Cu_{2.5}$ alloy and bimetallic sample.